Interpretive modelling of neutral particle fluxes generated by NBI ions in JET

V. Yavorskij[1,2], M. Cecconello[3], C. Challis[4], V. Goloborod'ko[1,2], V. Kiptily[4], M. Santala[5], S.E. Sharapov[4], P. de Vries[4], K. Schoepf [1] and JET-EFDA contributors*

JET-EFDA, Culham Science Centre, OX14 3DB, Abingdon, UK

[1]Institute for Theoretical Physics, University of Innsbruck, Association EURATOM-OEAW, Austria
[2]Institute for Nuclear Research, Ukrainian Academy of Sciences, Kiev, Ukraine
[3]Uppsala University, Association EURATOM-VR, Uppsala, Sweden
[4]Euratom/CCFE Fusion Association, Culham Science Centre, Abingdon, Oxon OX14 3DB, UK
[5]Helsinki University of Technology, Association Euratom-Tekes, FI-02015 TKK, Finland

* See Appendix of F. Romanelli et al., paper OV/1-3, this conference

e-mail:Victor.Yavorskij@uibk.ac.at

Abstract. Fluxes of neutral particles in the tens-keV energy range are emitted from JET plasmas and measured by a neutral particle analyzer (NPA) close to the plasma mid-plane with the line-of-sight perpendicular to the major axis of the torus. The experimental NPA data on the energy spectra of neutral fluxes allow for validation of both the model for beam ions and that for electron donors in tokamak plasmas. Our study aims at expounding JET NPA measurements of neutral particle fluxes generated by beam ions in a way that lets us conclude on beam ion transport and confinement. Employing both the 3D-Fokker-Planck code FIDIT for fast ions as well as a Monte-Carlo NPA code for bulk neutrals, we model the energy spectra of deuterium neutral fluxes detected by the NPA in JET in the energy range $5keV<E<120keV$. The simulation yields good quantitative agreement with the measurements in ICRH-free plasmas. Time-resolved NPA measurements confer useful information about the effect of MHD activity on fast beam ions. To exemplify that we consider a low I/low B JET discharge with a well pronounced NTM and fishbone activity. Analysis and modeling of NPA measurements in this discharge indicate that toroidally trapped fast ions are hardly affected by the modes and that the circulating ions are presumably redistributed or lost by the MHD modes.

1. Introduction

Fast ions confined in tokamak plasmas can be examined by analyzing energetic neutral particle fluxes emitted from the plasma, which are formed by these ions as a result of charge-exchange reactions with neutral atoms (electron donors) and recombination with plasma electrons [1]. In this way the toroidal field (TF) ripple induced degradation of the confinement of neutral beam injection (NBI) generated fast ions was investigated by measuring the neutral deuterium fluxes emitted from the plasma mid-plane using a neutral particle analyzer (NPA) in JET [1-6]. The effectiveness of neutral particle diagnostics for estimating the central ion temperature on ASDEX Upgrade with NBI heating was demonstrated in [7] and was also confirmed in the inspection of ICRH accelerated ions in Alcator C-Mod in [8]. A possibility of using the NPA diagnostics for ITER is discussed, for example, in [9].

On JET, fluxes of neutral particles in the tens-keV energy range are emitted from the plasma and measured by a neutral particle analyzer (NPA) with the line-of-sight in the mid-plane and perpendicular to the major torus axis (see Fig. 1).

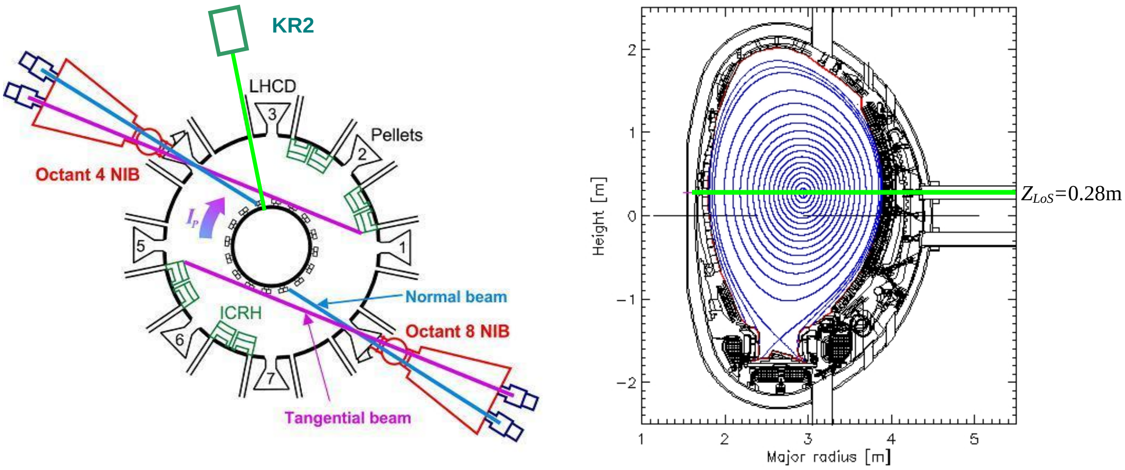

Fig. 1: Geometry of neutral beam injection and low-energy neutral particle analyser (KR2 NPA) on JET in toroidal (left) and poloidal cross-sections (right). The green line indicates the line-of-sight (LoS) of KR2.

The NPA experimental data on the energy spectra of neutral fluxes enable the validation of the models for both the beam ions and the electron donors in tokamak plasmas. Our study explains the energy spectra and magnitudes of neutral particle fluxes measured by NPA on JET for different beam ion confinement conditions. The involved time resolution of NPA measurements renders possible to consider the effects caused by MHD perturbations.

2. The model

To evaluate the NBI generated flux of fast neutrals detectable by NPA, $\Gamma_n(E)$, we determine first the differential rate of the corresponding emission of neutrals per volume, per energy and per pitch-angle. This emission rate contributing to the NPA signal may be expressed as

$$\frac{dR_{dn}(R,E)}{dVdEd\xi} = 2\pi\left[\sqrt{2E}\, f_d(R,Z,E,\xi)\, n_n(R,Z)\langle\sigma_{dn}u\rangle_E\right]\Big|_{Z=Z_{LoS},\xi=0} \quad (1)$$

where f_d denotes the beam deuteron distribution function, n_n the density of bulk neutrals and $\langle\sigma_{dn}u\rangle_E$ is the energy dependent speed averaged reaction parameter for the total neutralization interactions of deuterons with bulk neutrals, Z_{LoS} is the vertical coordinate of the NPA line of sight (Z_{LoS} = 28cm on JET as Fig. 1 shows) and $\xi = V_{\parallel}/V$ the deuteron pitch-angle cosine along the NPA line of sight ($\xi = 0$ on JET). Using Eqs. (1) the neutral deuterium flux Γ to the NPA can be calculated as

$$\Gamma(E) = \int dR d\Omega \frac{dR_{dn}(R,E)}{dVdEd\xi}\exp\left(-\int\frac{dR}{l}\right) = 2\pi\Delta\Omega\int dR\sqrt{2E}\, f_d(R,E,Z_{LoS},0)\, n_n(R,Z_{LoS})\langle\sigma_{dn}u\rangle_E \exp\left(-\int dR/l\right); \quad (2)$$

here Ω is the solid angle, $\Delta\Omega$ specifies a minute cone determined by the NPA aperture and l represents the "ionization" length of the neutral flux and is calculated by use of the total cross-section for electron loss [10]. Evidently, the neutral flux measured by the NPA in JET is directly determined by the beam deuteron distribution function in the mid-plane as well as by the distribution function of the bulk plasma neutral deuterium. For our calculations both the 3D-Fokker-Planck code FIDIT [3-6, 11] for fast NBI ions as well as a Monte-Carlo NPA code for bulk neutrals (based on the approach of [12, 13]) are employed. The Fokker-Planck model uses the classical Coulomb transport of beam ions induced by their orbital motions in JET including TF ripples but neglecting the effects of ICRH and MHD activity. The Monte-Carlo modeling of bulk neutrals assumes circular shape of the plasma cross-section [4,6] with an effective radius $a_{\text{eff}} \sim 1.5m$ chosen to provide the best agreement of modeled and measured fluxes of H^0 neutrals.

Referring to the constants-of-motion (COM) space variables E, r andλ, which denote the ion's energy, the maximum flux surface radius along the orbit and, respectively, the normalised magnetic moment ($\lambda=\mu B_0/E$), Fig. 2 compares the COM deuteron distributions $f_d(r,\lambda, E$=74keV) and $f_d(r,\lambda, E$=37keV) in JET resulting from 17.5MW injection of D^0 in the energy range 74keV< E<130 keV. The green lines represent deuterons contributing to the NPA signal, i.e. those with $V_{\|}$=0 at $Z = Z_{LoS}$ =0.28m. The red lines mark the boundaries of the

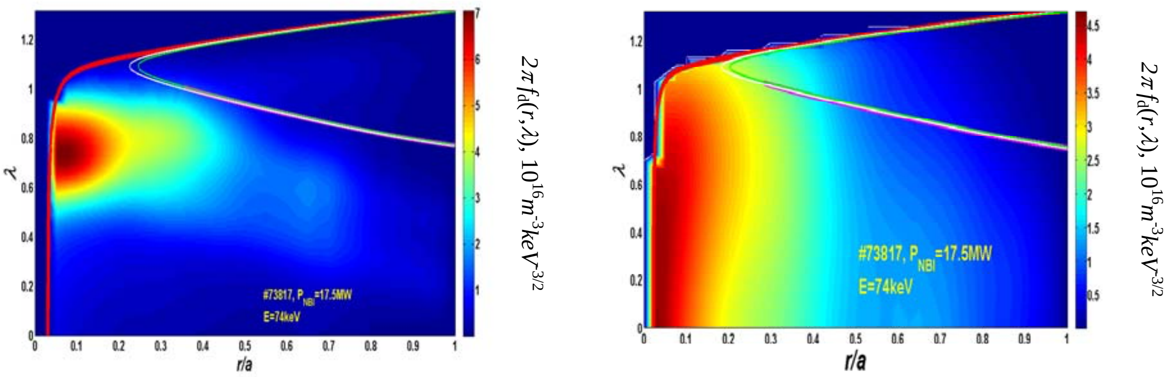

Fig. 2: Slices of the 3D COM distribution function of beam deuterons at energies E=74keV (left) and E=37keV (right) in the plane spanned by the normalized magnetic moment, $\lambda=\mu B_0/E$, and the maximum radial orbit coordinate, r, for 17.5MW D-NBI in JET (Pulse 73817). The green lines represent the deuterons contributing to NPA signal.

confinement domains of co-circulating and toroidally trapped particles, where the latter occur within a domain region bounded by white lines. The magenta lines indicate the separatrices between co-going (trapped and co-circulating) and counter-circulating orbits. Due to the proximity of the NPA LoS to the plasma midplane (Z_{ax}=0.3m), the deuterons contributing to the NPA signal originate from the well trapped ions and are adjacent to the white line separating the COM domains of trapped and passing ions. It is seen that the distribution of 74keV deuterons is strongly anisotropic in the longitudinal energy and localised in the plasma core with a maximum at $\lambda \approx 0.7$-0.8 and $r/a < 0.1$. Note that the majority of these deuterons are circulating ones and can not produce deuterium atoms detectable by NPA. Nevertheless the distribution of deuterons slowed down to 37keV is nearly isotropic in the longitudinal energy with a substantial population in the vicinity of the green line, i.e. with $V_{\|}$=0 along the NPA line of sight. On the LHS in Fig.3 we display the R, E-profile of the distribution $f_d(R, E,$

$Z= Z_{LoS}$, ξ=0) of those deuterons which produce D^0 neutrals contributing to the NPA signal. Evidently, the majority of these deuterons are produced as a result of pitch-angle scattering of high-energy beam deuterons. In accordance with the COM distributions of Fig. 2 the distribution $f_d(R,E,Z=Z_{LoS},\xi=0)$ is maximum in the plasma core $2.6m<R<3.4m$ and it decreases strongly for higher energies. The R,E- profile of the corresponding D^0 emission, $\sqrt{2E}\, f_d\left(R,E,Z_{LoS},0\right) n_n\left(R,Z_{LoS}\right)\left\langle \sigma_{dn} u\right\rangle_E \exp\left(-\int dR/l\right)$, that is detectable by the neutral particle analyzer on JET is illustrated on the RHS of Fig. 3. Due to attenuation of the neutral flux along the LoS, as described by the factor $\exp\left(-\int dR/l\right)$, and further, since the density of bulk neutrals, $n_n\left(R,Z_{LoS}\right)$, grows from its minimum value in the plasma core to its maximum

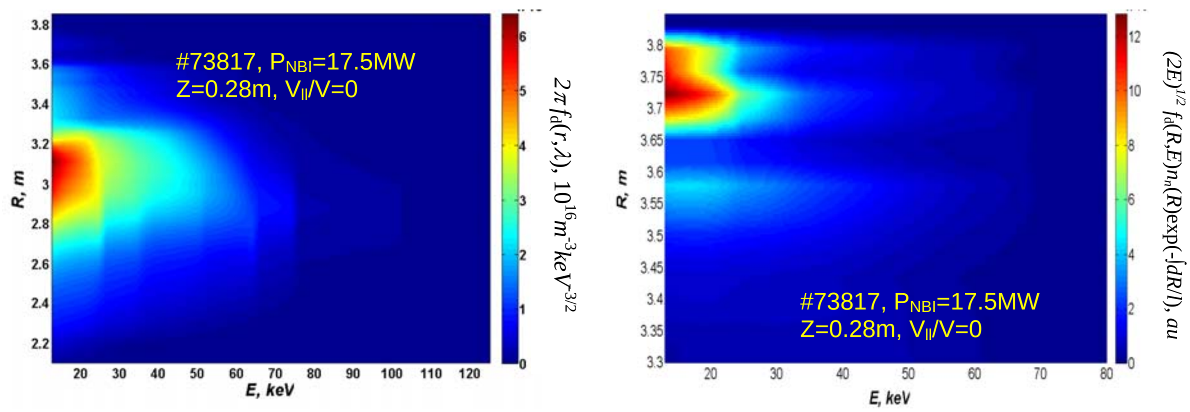

Fig. 3: R,E profiles of the distribution function of beam deuterons $f_d(R, E, Z= Z_{LoS}, \xi=0)$ (left) and of the rate of D^0 emission (right) detectable by NPA.

at the plasma edge, the majority of D^0 neutrals reaching the NPA is emitted from the low-B field area, $3.5m<R<3.8m$. Thus the fluxes of fast D^0 neutrals measured with the NPA at JET midplane will provide information mainly on the NBI generated ions confined at the low-B region of the plasma. Further, the RHS of Fig. 3 suggests that the emission of neutrals with energies E>25keV tends to become concentrated to the plasma core [14].

3. Energy spectra of NBI generated D^0 fluxes emitted from JET plasma: measurements and modeling

Here we consider the energy spectra of fluxes of D^0 with energies well above the temperature of bulk plasma deuterons [1] in ICRH-free JET plasmas. First we model the energy dependence of the D^0 flux emitted from a NBI heated plasma (pulse #73817, P_{NBI}=17.5MW). Figure 4 compares the modeled and measured D^0 fluxes Γ in the energy range $5keV<E<120keV$. The red curve depicts the measured spectrum of emitted deuterium neutrals while the black one represents the calculated spectrum. The simulation yields good quantitative agreement with the measurements in ICRH-free plasmas. Due to missing data on bulk deuterium neutrals the radial profile of the latter was modeled and fitted according to Figs. 5a and 5b. Calculating the neutrals' profile $N(r/a)$ for various effective plasma radii, the dotted black line in Fig.5a was seen to provide the best agreement of the modeled H^0 spectrum with the measured one as seen in Fig.5b.

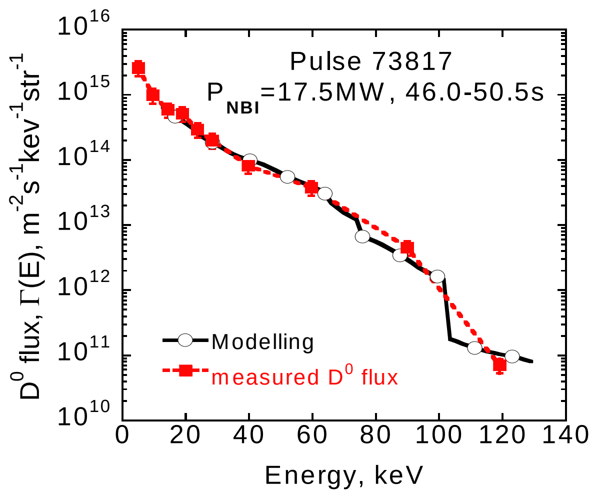

Fig. 4: Modeled and measured energy spectra of D^0 fluxes emitted from NBI heated JET plasma (Pulse 73817).

Recalling the production mechanisms of fast deuterium neutrals, a deterioration of the confinement of beam deuterons should essentially result in weakening of the D^0 fluxes. Accordingly, in JET ripple experiments where an additional *N*=16 TF ripple harmonic was introduced to investigate its effect on the performance of ELMy H-mode plasmas [15], a reduction of the fluxes of deuterium neutrals emitted from the plasma mid-plane was observed in the 5*keV*<*E*<40*keV* energy range. When the magnitude of the *N*=16 TF ripple harmonic was about 1% at the outer part of the plasma, the maximum ripple induced reduction of the fluxes was ~ 50% at energies *E* > 30keV [3]. In Fig. 6 we display the measured and modelled D^0 fluxes in two ICRH-free positive shear JET plasmas with very similar parameters (see Fig. 7) but one without and the other with the additional *N*=16 TF ripple harmonic. The modelled D^0 fluxes in Fig. 6 consist of parts produced by neutralization of beam ions as well as of Maxwellian bulk deuterons. In both

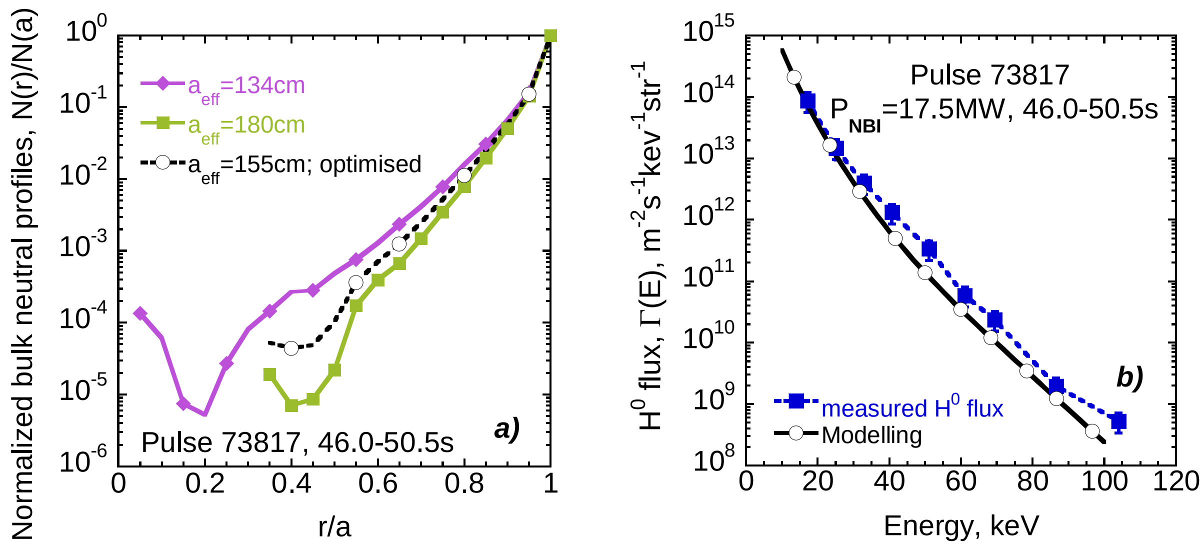

Fig. 5 Monte-Carlo modeled density profiles of bulk D^0 neutrals (a). The optimised profile (a_{eff}=155cm) in Fig.5a provides the best correspondence of the modeled H^0 spectrum with the measured one in Fig.5b. This profile is used for calculation of the D^0 spectra in Fig. 4.

discharges a predominantly perpendicular (see Fig. 1) deuterium NBI with 7.5MW power was applied for plasma heating. As evident from Fig. 6 (solid lines with marks), a 1%

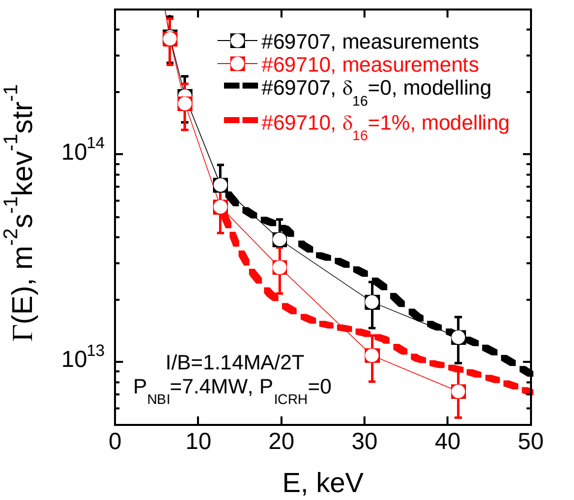

Fig. 6: Measured and modeled D^0 fluxes in JET plasmas without (Pulse #69707, $\delta_{16}=0$) and with (Pulse #69710, $\delta_{16}=1\%$) N=16 TF ripple harmonic.

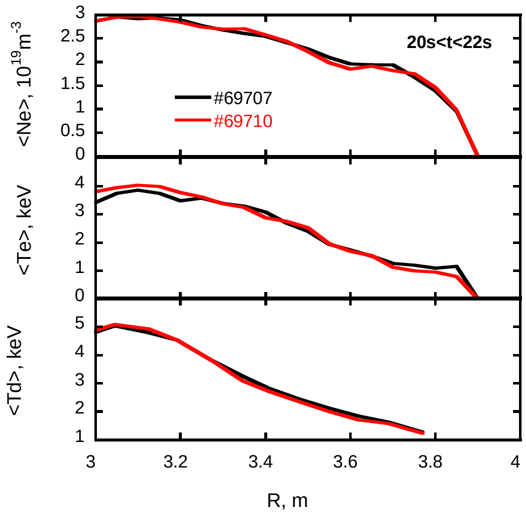

Fig. 7: Basic plasma parameters averaged over the time interval 20s<t<22s which corresponds to the NPA measurements in Fig. 6.

additional ripple magnitude effects a nearly 50% drop in the D^0 flux measured at 30keV<E<40keV, which is in qualitative agreement with the modelled reduction in the flux of deuterium neutrals (dashed lines in Fig.6). The deviation of modelled fluxes from the measured ones at energies 20keV<*E*<30keV is of the order of errors in the experimental data. A reason for discrepancy may be the simplified model of bulk neutrals that does not account consistently for the real shapes of the plasma and the first wall.

It should be pointed out that, in spite of the weak effect of TF ripples on the bulk plasma confinement, the beam deuterons contributing to the NPA signal are significantly affected by ripple induced transport [3,4,6]. This is due to the sensitivity of beam ions with $V_{||} \sim 0$ at $Z = Z_{LoS}$ to ripple perturbation of the magnetic field. Those ions are mainly produced as a result of pitch-angle scattering of passing injected deuterons into toroidally trapped orbits. In the standard JET configuration without additional *N*=16 TF ripple harmonic ($\delta_{16}=0$) and at a low amplitude of MHD activity those ions are well confined because of the relatively low radial transport associated with neoclassical diffusion. Enhanced ripples can substantially affect the confinement of toroidally trapped beam ions due to a strong ripple induced stochastic diffusion if the ripple magnitude exceeds the Goldston-White-Boozer threshold, $\delta > \delta_{GWB}$, [16] or as a result of a collisional superbanana diffusion if $\delta < \delta_{GWB}$ [17]. Note that stochastic diffusion plays a substantial role at the periphery of the low-*B* part of the plasma, whereas superbanana diffusion is significant in the plasma core.

Expectedly, the midplane NPA measurements on JET could be efficient also for inspecting toroidally trapped ions in ICRH heated plasmas as well as in those with MHD activity. The time-resolved NPA measurements can confer useful information about the effect of MHD activity on fast beam ions. To exemplify that we consider a low I/low B JET discharge with a

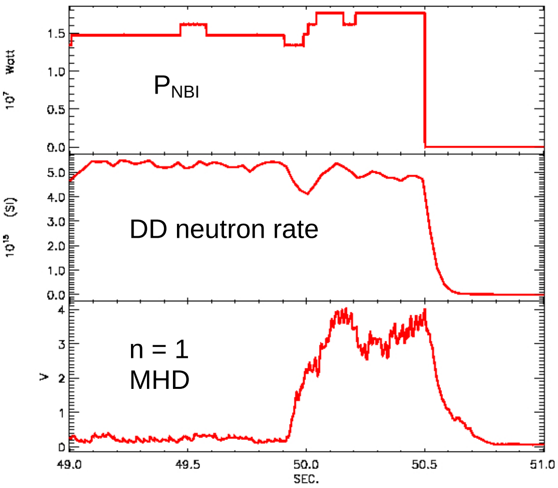

Fig. 8: Time traces of P_{NBI}, DD neutron rate and n=1 MHD activity. Pulse 73821 (I/B = 1.1MA/1.35T)

large-amplitude MHD activity during high power NBI operation, P_{NBI}, as detailed in Figs. 8 and 9. The well pronounced neoclassical tearing modes (NTM) and fishbones seemingly prevent an increase of the DD neutron rate, which should have resulted from the 2.5 MW augmentation of the NBI power. On the other hand, the NPA measurements displayed in Fig. 10a show for that an expected increase of the fluxes of energetic D^0 neutrals. Note that this increase is in remarkable agreement with our modeling neglecting MHD effects (Fig. 10b). Taking into account that the NPA on JET detects only neutrals produced by fast ions with $V_{||} \sim 0$, we conclude that toroidally trapped fast ions are hardly affected by the modes. Therefore, for explaining the neutron rate observed, the confined circulating ions have to be redistributed or lost by the MHD modes.

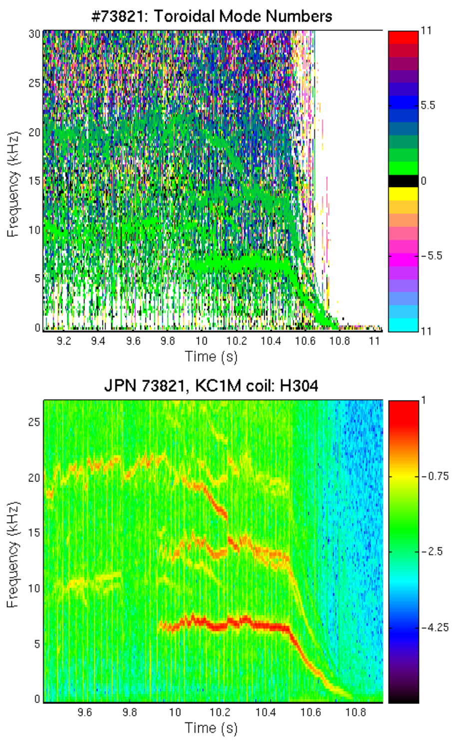

Fig. 9: Spectrograms showing the MHD mode evolution. Pulse 73821 (I/B = 1.1MA/1.35T)

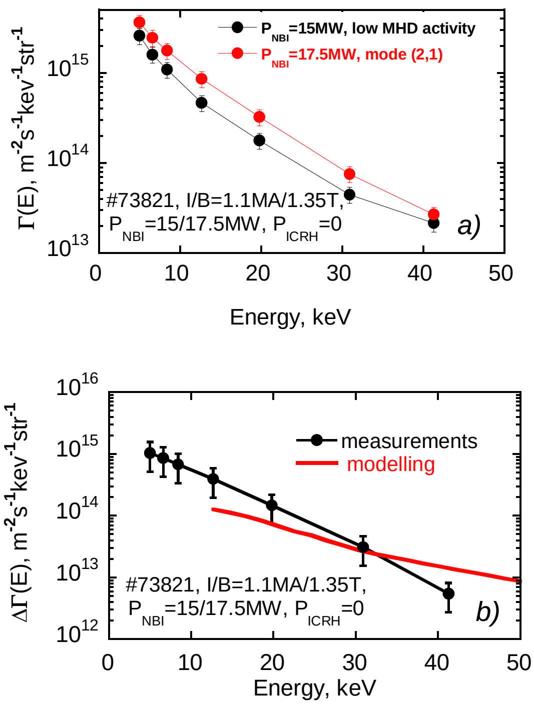

Fig. 10: (a) Measured D^0 fluxes before and during MHD activity. (b) Modeled and measured increase of $\Gamma(E)$ due to 2.5MW increase of P_{NBI} in shot 73821.

4. Conclusion

Our study confirms the validity of NPA analysis of energetic hydrogen-like neutrals escaping from the plasma as a diagnostic tool of NBI ions. Thus NPA measurements of the energy spectra of fast neutrals emitted near the JET plasma midplane enable the examination of the loss mechanisms of energetic charged particles. This applicability was clearly demonstrated for TF ripple losses of beam ions in JET. The corresponding measurements provide a valuable database for the validation of ripple loss mechanisms as well as of the models for fast ions confined in tokamak plasmas. A satisfactory agreement between the data and the Fokker-Planck code FIDIT used for describing the beam ions in ICRH-free JET plasmas was found. We point out that a similar interpretive modelling of NBI generated neutral fluxes in the presence of ICRH will allow for examining the effect of ion cyclotron heating on the fast ion energy distribution. The NPA measurements on JET could be efficient also for the inspection of the effect of MHD activity on toroidally trapped fast ions.

Acknowledgement

This work, supported by the European Communities under the contract of Association between EURATOM/ÖAW, was carried out within the framework of the EFDA Agreement. The views and opinions expressed herein do not necessarily reflect those of the European Commission.

References

[1] TUBBING, B., Proc. 22 EPS Conf. on Contr. Fus. Plasma Phys. Vol. 19C, p. IV-001 (1995)
[2] JACQUINOT, J., J. Nucl. Fusion **38**, (1998) 1263
[3] YAVORSKIJ, V., *et al.*, 33rd EPS Plasma Physics Conference, Rome, p. P-2.037 (2006).
[4] YAVORSKIJ, V., *et al.*, 34th EPS Plasma Physics Conference, Warsaw, P2.041 (2007).
[5] SCHOEPF, K., *et al.*, Proc. Burning Plasma Diagnostics, Varenna, 2007, p 331
[6] GOLOBOROD'KO, V., *et al.*, 10th IAEA TM on Energetic Particles, Kloster Seeon, Germany, P11 (2007)
[7] KURKI-SUONIO, T., *et al*., Plasma Phys. Contr. Fusion, **44** (2002) 475
[8] LEE, W.D., *et al*., Plasma Phys. Contr. Fusion, **45** (2003) 1465
[9] LOARTE, A., *et al*., Nucl. Fusion **47** (2007) S203–S263
[10] KOROTKOV, A.A., JANEV, R.K., 1996 *Phys. Plasmas* **3** 1512
[11] HAWKES, N., *et al*., Plasma Phys. Control. Fusion **47** (2005) 1475.
[12] HUGHES M. H., Post, D. E., J. Comp. Phys. **28** 43 (1978).
[13] DELIANG, Yu., *et al.*, Plasma Science and Technology **9** 133 (2007).
[14] AFANASYEV, V., *et al.*, Rev. Sci. Instrum., **74**, (2003) 2338
[15] PARAIL, V., *et al.*, Proc. 32 EPS Conf. on Plasma Phys. Vol. 29C, p. O-2.008 (2005)
[16] GOLDSTON, R.B., *et al.*, Phys. Rev. Lett. **47** (1981) 647
[17] YAVORSKIJ, V., *et al.*, Physics of Plasmas **6** (1999) 385